Surface Plasmon Resonance Imaging Measurements of Electrostatic Biopolymer Adsorption onto Chemically Modified Gold Surfaces

Claire E. Jordan and Robert M. Corn*

Department of Chemistry, University of Wisconsin—Madison, 1101 University Avenue, Madison, Wisconsin 53706

A combination of in situ and ex situ surface plasmon resonance (SPR) imaging experiments is used to characterize the differential electrostatic adsorption of proteins and synthetic polypeptides onto photopatterned monolayers at gold surfaces. The nonspecific electrostatic adsorption of proteins onto negatively charged self-assembled monolayers (SAMs) of 11-mercaptoundecanoic acid (MUA) is found to depend on the protein pI, solution ionic strength, and solution pH. The pH dependence of the electrostatic adsorption of the protein avidin onto a MUA SAM indicates that a full monolayer adsorbs at a solution pH greater than 5.0, and an "effective pK_a" of 3.6 is determined for the avidin adsorption. This effective pK_a is a combination of the pK_a of the MUA monolayer and the ion pairing adsorption coefficient for the avidin. Additional SPR imaging experiments show that the electrostatic adsorption of the synthetic polypeptide poly-L-lysine (PL) onto a MUA SAM varies with molecular weight, forming a full PL monolayer for polypeptides with more than 67 lysine residues.

The nonspecific electrostatic adsorption of proteins and polypeptides onto charged surfaces occurs frequently in biological membrane systems.[1−3] This process also serves as the basis for a variety of bioanalytical sensor devices and affinity chromatography schemes at metal and oxide surfaces.[4−8] In some instances, the nonspecific electrostatic adsorption of proteins can overwhelm any specific covalent or hydrogen bonding interactions with the surface and must be minimized. At gold surfaces, one effective way to control the adsorption of proteins and polypeptides is to chemically modify the interface by the self-assembly of an alkanethiol monolayer.[9−12] For example, alkanethiol self-as-

sembled monolayers (SAMs) terminated with poly(ethylene glycol) groups have been used to prevent the nonspecific adsorption of proteins at gold surfaces,[13] and SAMs that are terminated with a charged functional group as well as other charged surfaces have been used to create electrostatically adsorbed polypeptide monolayers[14,15] and even multilayers.[16−18]

In a series of previous papers,[15,19,20] we have used monolayers of the synthetic polypeptide poly-L-lysine (PL) to control the adsorption of proteins onto vapor-deposited gold films. The PL monolayers are adsorbed onto SAMs of 11-mercaptoundecanoic acid (MUA) either by electrostatic interactions (ammonium—carboxylate ion pairs) or by covalent amide bond formation and have been characterized with a combination of polarization—modulation FT-IR reflection—absorption spectroscopy (PM/FT-IR/RAS) and surface plasmon resonance (SPR) thickness measurements. A schematic diagram of the scanning SPR apparatus used previously is shown in Figure 1. In these experiments, the reflectivity of a thin (47 nm) vapor-deposited gold film attached to a prism is monitored with a HeNe laser (λ = 632.8 nm) as the angle of incidence (θ) is varied. The reflectivity is recorded as a function of incident angle and exhibits a sharp minimum just beyond the critical angle. At this reflectivity minimum (denoted as the SPR angle), surface plasmon polaritons are created on the opposite side of the thin gold film. Any changes in the thickness or index of refraction of the material adsorbed onto the gold surface results in a shift of the SPR angle, which can be readily detected and quantified.[15,21−23] The SPR angle shift measurement has been used frequently to monitor adsorption onto noble metal surfaces[24−26] and is the basis of the Biacore SPR adsorption instrument currently manufactured by Pharmacia.[27]

(1) Dryhurst, G.; Kadish, K. M.; Scheller, F.; Renneberg, R. *Biological Electrochemistry*; Academic Press: New York, 1982.
(2) Roth, C. M.; Lenhoff, A. M. *Langmuir* **1995**, *11*, 3500−3509.
(3) Elgersma, A. V.; Zsom, R. L. J.; Norde, W.; Lyklema, J. *J. Colloid Interface Sci.* **1990**, *138*, 145−156.
(4) Cass, A. E. G., Ed. *Biosensors, A Practical Approach*; Oxford University Press: New York, 1990.
(5) Decher, G.; Lehr, B.; Lowack, K.; Lvov, Y.; Schmitt, J. *Biosens. Bioelecton.* **1994**, *9*, 677−648.
(6) Turner, A. P. F., Karube, I., Wilson, G. S., Eds. *Biosensors: Fundamentals and Applications*; Oxford University Press: Oxford, 1987.
(7) Porath, J.; Olin, B. *Biochemistry* **1983**, *22*, 1621−1630.
(8) Smith, M. C.; Furman, T. C.; Pidgeon, C. *Inorg. Chem.* **1987**, *26*, 1965−1969.
(9) Leggett, G. J.; Roberts, C. J.; Williams, P. M.; Davies, M. C.; Jackson, D. E.; Tendler, S. J. B. *Langmuir* **1993**, *9*, 2356−2362.
(10) Prime, K. L.; Whitesides, G. M. *Science* **1991**, *252*, 1164−1167.
(11) Tarlov, M. J.; Bowden, E. F. *J. Am. Chem. Soc.* **1991**, *113*, 1847−1849.
(12) Schneider, T. W.; Buttry, D. A. *J. Am. Chem. Soc.* **1993**, *115*, 12391−12397.
(13) Prime, K. L.; Whitesides, G. M. *J. Am. Chem. Soc.* **1993**, *115*, 10714−10721.
(14) Blaakmeer, J.; Cohen-Stuart, M. A.; Fleer, G. J. *J. Colloid Interface Sci.* **1990**, *140*, 314−325.
(15) Jordan, C. E.; Frey, B. L.; Kornguth, S.; Corn, R. M. *Langmuir* **1994**, *10*, 3642−3648.
(16) Lvov, Y.; Ariga, K.; Ichinose, I.; Kunitake, T. *J. Am. Chem. Soc.* **1995**, *117*, 6117−6123.
(17) Lvov, Y.; Decher, G.; Sukhorukov, G. *Macromolecules* **1993**, *26*, 5396.
(18) Cooper, T. M.; Campbell, A. L.; Crane, R. M. *Langmuir* **1995**, *11*, 2713−2718.
(19) Frey, B. L.; Corn, R. M. *Anal. Chem.* **1996**, *68*, 3187−3193.
(20) Frey, B. L.; Jordan, C. E.; Kornguth, S.; Corn, R. M. *Anal. Chem.* **1995**, *67*, 4452−4457.
(21) Economou, E. N. *Phys. Rev.* **1969**, *182*, 539−554.
(22) Pockrand, I. *Surf. Sci.* **1978**, *72*, 577−588.
(23) Swalen, J. D.; Gordon, J. G. I.; Philpott, M. R.; Brillante, A.; Pockrand, I.; Santo, R. *Am. J. Phys.* **1980**, *48*, 669−672.
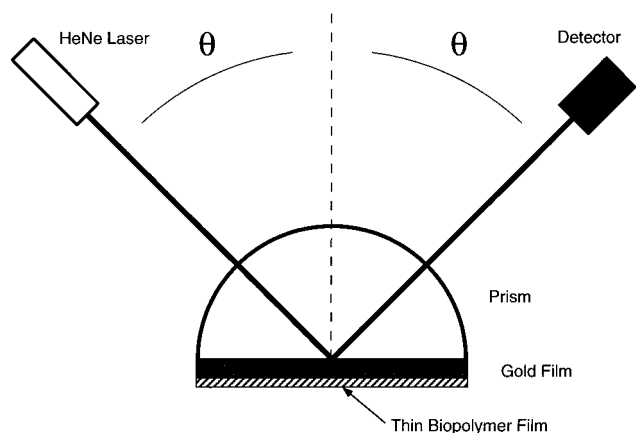(24) Siirila, A. R.; Bohn, P. W. *Langmuir* **1991**, *7*, 2188−2194.

Figure 1. Optical layout for an SPR scanning instrument. p-Polarized light from a HeNe laser is directed at a hemispherical prism, to which the sample is attached. The sample consists of a vapor-deposited thin gold film, the biopolymer adsorption onto which is measured. In the scanning setup, the reflected intensity from the prism sample assembly is measured as a function of incident angle θ using a photodiode detector.

Figure 2. Optical layout for the SPR imaging instrument. A HeNe laser is sent through a spatial filter and beam expander, which are required so that the entire sample surface can be illuminated. This expanded beam is then directed at the prism sample assembly. A 47 nm thick gold film vapor-deposited onto a glass slide is used as the sample substrate for the formation of patterned self-assembled monolayer (SAM) films. This is in contact with a 60° prism, which is required in order to couple the incident p-polarized light into the surface plasmon modes at the interface. In the imaging setup, the reflected intensity at some fixed angle is then measured across the beam using a CCD camera. For in situ experiments, a flow cell is attached to the back of the prism sample assembly so that the gold sample is in contact with solution. An image of a photopatterned SAM array obtained with this instrument is also shown.

In addition to the scanning SPR technique, fixed-angle SPR imaging can also be employed to measure the electrostatic adsorption of biopolymers onto photopatterned alkanethiol SAMs. SPR imaging and microscopy have been used previously by various researchers to study biopolymer adsorption onto patterned surfaces.[28-30] A schematic diagram of the SPR imaging apparatus is shown in Figure 2. In this experiment, an expanded HeNe laser beam is reflected through a prism off of a thin gold film near the SPR angle and detected with a CCD camera to produce images such as that shown in the figure. Any changes in the index of refraction or the thickness of a film adsorbed onto the gold surface result in changes in the intensity of the reflected light at a fixed angle. By creating two different alkanethiol SAMs with UV photopatterning on a single thin gold film, a differential adsorption measurement can be performed by monitoring changes in the SPR image as the sample is exposed to a solution of interest. These differential adsorption measurements are equal in sensitivity to the SPR angle shift measurements of biopolymer adsorption performed previously with the scanning SPR instrument. The SPR imaging technique can be used to monitor the adsorption of submonolayer amounts of material in both ex situ and in situ configurations. In this article, SPR imaging differential adsorption measurements are employed to examine how the pI of a protein or polypeptide, its molecular weight, the solution pH, and the electrolyte concentration can affect the electrostatic adsorption of a biopolymer onto a chemically modified gold surface.

EXPERIMENTAL CONSIDERATIONS

Materials. 11-Mercaptoundecanoic acid (MUA; Aldrich), L-lysine (Aldrich), Lys-Lys:HCl (Sigma), poly-L-lysine:HBr (PL, MW 531, 1000,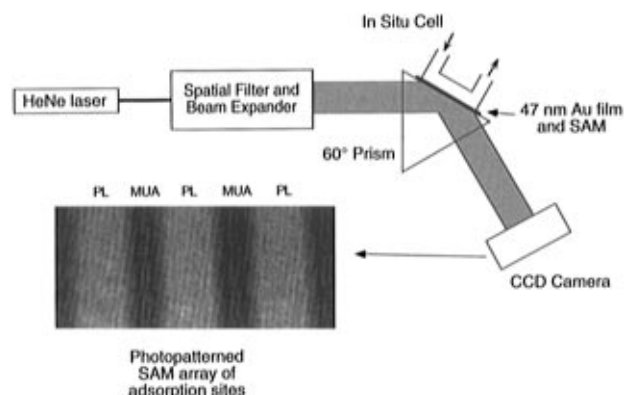 4000, 9000, 14 000, 23 800, 58 000; Sigma), avidin (Sigma), α-acid glycoprotein (α-AGP; Sigma), NaHCO₃ (Fluka), Na₂HPO₄ (Fluka), and absolute ethanol (Pharmco) were all used as received. 11-Mercaptoundecanol (MUD) was synthesized according to a procedure outlined previously.[31] Millipore filtered water was used for all aqueous solutions and rinsing.

Surface Preparation, Monolayer Formation, and Photopatterning. The SPR experiments utilized thin (47 nm) gold films that had been vapor-deposited onto BK7 or SF10 glass slides (18 × 18 mm²) as described previously.[31,32] Alkanethiol monolayers of either MUA or MUD were formed on the gold films by immersing the surface into a 1 mM ethanolic solution for at least 18 h, followed by a thorough rinsing with both ethanol and water. Photopatterning of the samples was performed by irradiating the samples with a mercury arc lamp (Oriel) for 5 h. For ex situ experiments, solutions of avidin (0.44 μM) and α-AGP (1.1 μM) in 5 mM NaHCO₃, pH = 8, were used, and deposition times were about 30 min. Avidin adsorption for the in situ studies of ionic strength dependence was from the same solution as above, and the images were taken in 5 mM NaHCO₃. For the in situ pH dependence experiments, avidin was adsorbed from solutions of 0.44 μM avidin in 10 mM Na₂HPO₄, and the pH was adjusted with NaOH and HCl. Images for the pH experiments were obtained in these avidin solutions. Solutions used in the molecular weight dependence study of PL all had a constant 0.7 mM lysine residue concentration in 5 mM NaHCO₃, pH $\approx$ 8, and the amount of adsorbed PL was obtained by analyzing images of the sample taken in these PL solutions.

SPR Imaging Experiments. Both scanning SPR measurements (Figure 1) and SPR imaging experiments (Figure 2) are described in this paper. The scanning SPR apparatus has been described in detail in previous papers[15,31] and generates plots (denoted as SPR curves) of the percent reflectivity (%R) as a

(25) Spinke, J.; Liley, M.; Schmitt, F. J.; Guder, H. J.; Angermaier, L.; Knoll, W. *J. Chem. Phys.* **1993**, *99*, 7012−7019.

(26) Drake, P. A.; Bohn, P. W. *Anal. Chem.* **1995**, *67*, 1766−1771.

(27) Löfås, S.; Malmqvist, M.; Rönnberg, I.; Stenberg, E.; Liedberg, B.; Lundström, I. *Sens. Actuators B* **1991**, *5*, 79−84.

(28) Fischer, B.; Heyn, S. P.; Egger, M.; Gaub, H. E. *Langmuir* **1993**, *9*, 136−140.

(29) Rothenhäusler, B.; Knoll, W. *Nature* **1988**, *332*, 615−617.

(30) Schmitt, F.-J.; Knoll, W. *Biophys. J.* **1991**, *60*, 716−720.

(31) Frey, B. L.; Hanken, D. G.; Corn, R. M. *Langmuir* **1993**, *9*, 1815−1820.

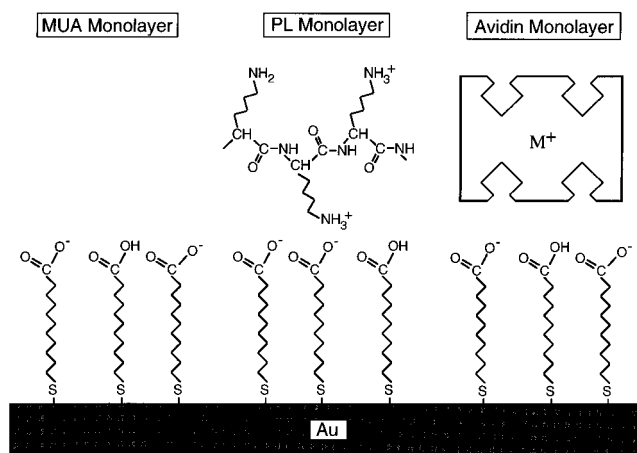(32) Hanken, D. G.; Corn, R. M. *Anal. Chem.* **1995**, *67*, 3767−3774.

Figure 3. Schematic diagram of three monolayers adsorbed onto a gold substrate: a negatively charged 11-mercaptoundecanoic acid (MUA) monolayer, a positively charged poly-L-lysine (PL) monolayer electrostatically adsorbed onto MUA, and the protein avidin electro-statically adsorbed to MUA.

Figure 4. SPR reflectivity and differential reflectivity curves for PL and avidin monolayers measured ex situ. (a) Experimental and theoretical SPR reflectivity curves measured on PL and avidin surfaces. The circles and squares show respectively the experimental percent reflectivities for PL and avidin monolayers measured as a function of incident angle θ. The solid and dotted lines are the results of four-phase complex Fresnel calculations for PL and avidin films, and the shift in the angle of minimum $\%R$ is due to the difference in thickness between the two monolayers. (b) Experimental and theoretical differential reflectivity curves obtained from the difference in the SPR curves in (a) for PL and avidin monolayers.

function of incident angle θ. The SPR curves shown in this paper were obtained from a slightly modified scanning SPR instrument that used a CCD camera as the photodetector. The SPR imaging experiments were performed with an instrument that contained a 1 mW HeNe laser (Newport Corp.), a spatial filter and beam expander (Newport Corp. Model 900, with a 10 μm pinhole and 50× objective), and a CCD camera (Panasonic Model WV BL200). Samples were introduced into the imaging apparatus by attaching the back of the gold-coated glass slides to a coupling prism with index matching fluid. The ex situ experiments used a 45° BK7 ($n = 1.515$) glass prism with methyl salicylate (Aldrich) as the index matching fluid; for the in situ measurements, a 60° SF10 ($n = 1.727$) glass prism with $n = 1.725$ index matching fluid (Cargille) was employed. The reflected intensity across the beam is then measured to obtain images such as that shown in Figure 2. These images can be represented quantitatively by line profiles which are generated by averaging together the pixel values from each column of the CCD camera. For the in situ experiments, a Teflon flow cell with a 60 μL volume is attached to the prism/sample assembly so that a 2 cm^2 area of the chemically modified gold surface is in contact with solution.

RESULTS AND DISCUSSION

Ex Situ SPR Imaging Experiments of Protein Adsorption. SPR imaging experiments performed at a single fixed angle are employed in this paper to monitor differences in biopolymer adsorption onto photopatterned, chemically modified gold surfaces. For example, a negatively charged MUA monolayer can be used to electrostatically adsorb the polycation poly-L-lysine or any positively charged protein, such as avidin (see Figure 3). One method of determining the difference in thickness between the PL monolayers and the avidin monolayers formed by this electrostatic adsorption process is to measure the different SPR angle shifts obtained from ex situ scanning SPR experiments. Figure 4a plots the experimental and theoretical SPR curves for such a pair of measurements. The circles in the figure correspond to the experimental SPR curve obtained from a PL monolayer, and the squares are the experimental data from an avidin monolayer. The solid and dotted lines are theoretical fits of the
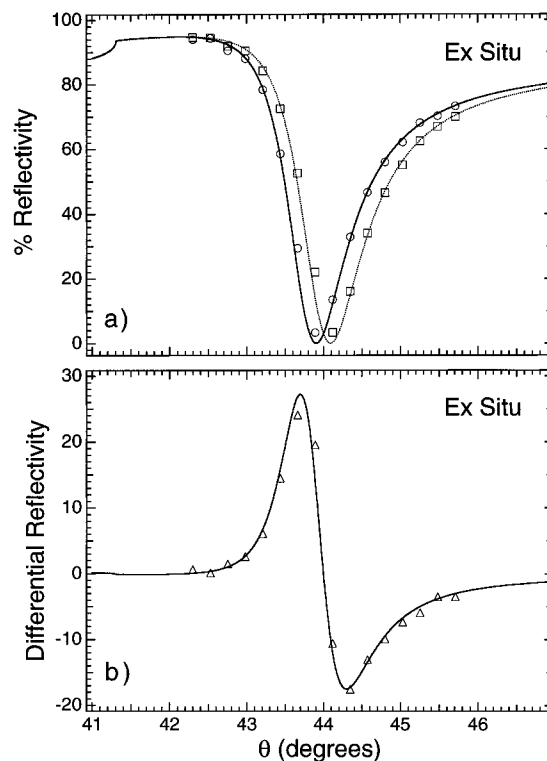
data obtained from four-phase complex Fresnel calculations.[33] A difference of 0.184° in the SPR angle is observed for the two monolayers, as expected from previous results.[20] In addition to the SPR angle shift, the change in $\%R$ at a fixed angle near the SPR minimum can be used to quantitate the difference in thickness between the two monolayers. Figure 4b plots the differential reflectivity curve, which is simply the difference in the two observed $\%R$ values as a function of incident angle. A maximum in the differential reflectivity is observed just below the SPR angle; SPR imaging experiments are typically performed at this angle to obtain the highest sensitivity to changes in the thickness or index of refraction of the adsorbed material.

To perform differential adsorption measurements with the SPR imaging apparatus, two-component surfaces are created that consist of alternating stripes of two different surface functional groups. These surfaces are prepared by a series of adsorption/self-assembly, photochemical desorption, and rinsing steps. For example, the procedure required for the formation of surfaces with stripes of both PL and MUA monolayers (MUA/PL surface), used for all protein differential adsorption experiments, is shown in Figure 5. First, a SAM of MUA was formed on a gold surface, after which PL was electrostatically adsorbed onto the MUA as described previously.[15] After formation of the PL−MUA bilayer, the surface was placed behind a mask and irradiated with UV

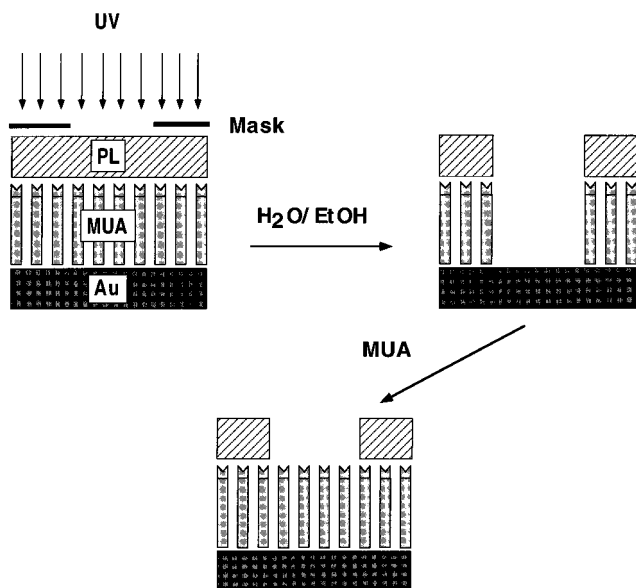(33) Hansen, W. N. *J. Opt. Soc. Am.* **1968**, *58*, 380−390.

Figure 5. Schematic diagram outlining the process for making patterned MUA and PL surfaces. Initially, MUA is adsorbed onto the gold surface from an ethanolic solution, and PL is electrostatically bound to the MUA. This PL monolayer is then placed behind a mask and exposed to UV light. The UV light oxidizes the gold−sulfur bond so that both the MUA and the PL can be removed in the exposed areas by rinsing with water and ethanol. MUA can then be readsorbed to the exposed gold, creating a surface containing areas of MUA and areas of PL, which is used to study differential protein adsorption.

Figure 6. Line profiles showing the adsorption of avidin and α-acid glycoprotein onto patterned MUA/PL surfaces. The solid lines in both (a) and (b) are the percent reflectivities measured for gold samples photopatterned with stripes of PL and MUA. The dotted line in (a) is the %R measured after exposing the sample to a pH = 8.5 avidin solution and subsequently rinsing with water. The adsorption of α-AGP at pH = 8.5 onto a MUA/PL sample is shown by the dotted line in (b).

light. The UV irradiation causes the gold−sulfur bond to be oxidized,[34,35] so that both the MUA and PL layers are removed from the exposed stripes by rinsing with ethanol and water. This photopatterned surface is then re-exposed to an ethanolic MUA solution, resulting in a surface with alternating regions of MUA and PL monolayers. At a neutral or slightly basic pH, the areas of PL will be positively charged, and those of MUA will be negatively charged; this surface can thus be used to examine the electrostatic adsorption of proteins. When the reflectivity from such a surface is measured in an SPR imaging experiment at a fixed angle, images of the type shown in Figure 2 are obtained. These images are represented quantitatively by averaging the %R values measured at each pixel of the CCD camera along the stripes and generating a line profile across the image.

For example, line profiles generated from SPR images of two MUA/PL surfaces are plotted as the solid lines in Figure 6. The SPR images were obtained at an incident angle below the SPR angle, and the line profiles from these images show that the %R from the PL monolayer is higher than that from the MUA monolayer, as expected since it is thicker by 10.5 Å.[15] This surface should contain both negatively charged MUA regions and positively charged PL regions when exposed to an aqueous solution of pH = 8. The dotted lines in Figure 6 are the line profiles for two such surfaces that have been exposed to solutions of either avidin (pI = 10) or α-acid glycoprotein (α-AGP, pI = 3). The surfaces have been removed from the adsorption solution and rinsed with a water solution before being imaged. From these ex situ measurements, it is evident that the avidin nonspecifically
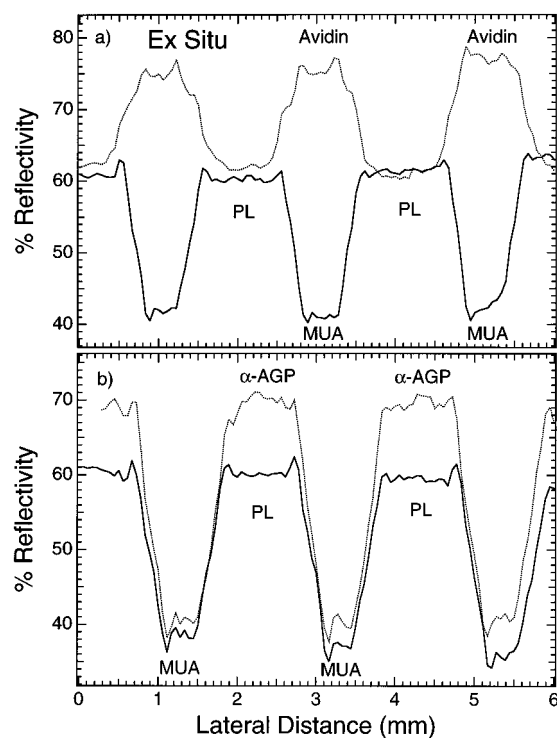
(34) Tarlov, M. J.; Burgess, D. R. F.; Gillen, G. *J. Am. Chem. Soc.* **1993**, *115*, 5305−5306.

(35) Huang, J.; Dahlgren, D. A.; Hemminger, J. C. *Langmuir* **1994**, *10*, 626−628.

binds to the MUA regions of the surface and that the α-acid glycoprotein nonspecifically binds to the PL regions of the surface. Thus, the nonspecific adsorption of these two proteins appears to be dominated by the electrostatic interactions between the proteins and the surface functional groups.

While, in principle, this information could have been obtained from a series of scanning SPR measurements, the SPR imaging technique is a rapid and very sensitive method for studying protein adsorption. The speed and sensitivity of these experiments arise from the fact that adsorption onto a single surface containing multiple areas with different functional groups can be measured simultaneously. Very small changes in %R corresponding to submonolayer amounts of biopolymer adsorption can be observed with this measurement, and if the data are normalized (as in Figure 6) to obtain quantitative %R values, an effective thickness can be determined from the data.

In Situ SPR Imaging Experiments of Protein Adsorption. The same SPR imaging experiments that were performed ex situ on the adsorption of avidin onto MUA/PL surfaces can also be performed in situ with the photopatterned monolayers in contact with an avidin adsorption solution. As in the previous section, a comparison of the SPR curves obtained from in situ scanning SPR measurements for PL and avidin monolayers can help to quantitate the changes in %R expected from an in situ SPR imaging experiment. Figure 7 plots the SPR reflectivity curves and differential reflectivity curves for these two monolayers in an in situ cell utilizing an SF10 coupling prism. As shown in the figure, the SPR minima have shifted to higher angles, and the SPR reflectivity curves have broadened. This broadening leads to a
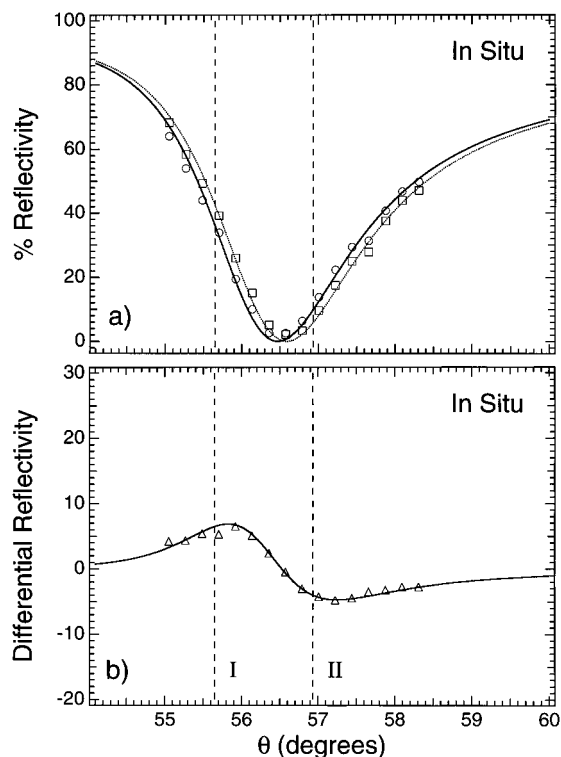
Figure 7. SPR reflectivity and differential reflectivity curves for a PL monolayer and an avidin monolayer measured in situ. (a) The circles and the solid line show the experimental and theoretical SPR curves for a PL monolayer, and the squares and dotted line show the same for an avidin monolayer. Notice that, when measured in situ, the SPR reflectivity curves are shifted to higher angles and are considerably broadened compared to the ex situ SPR curves shown in Figure 4a for the same monolayers. (b) The differential reflectivity resulting from the SPR curves in (a); notice here that the differential reflectivities are much less than those in Figure 4b. The dashed lines labeled I and II correspond to the two angles at which the lines in Figure 8 were generated.

Figure 8. Differential reflectivity vs change in thickness of a thin film, with refractive index of 1.45, calculated in situ at two fixed angles shown as I and II in Figure 7. The solid line is the differential reflectivity at angle I and shows a region of about 50 Å for which the differential reflectivity changes linearly with thickness before it starts to level out. The dashed line is the differential reflectivity at angle II and is an example of an angle where the differential reflectivity first decreases with increasing thickness.
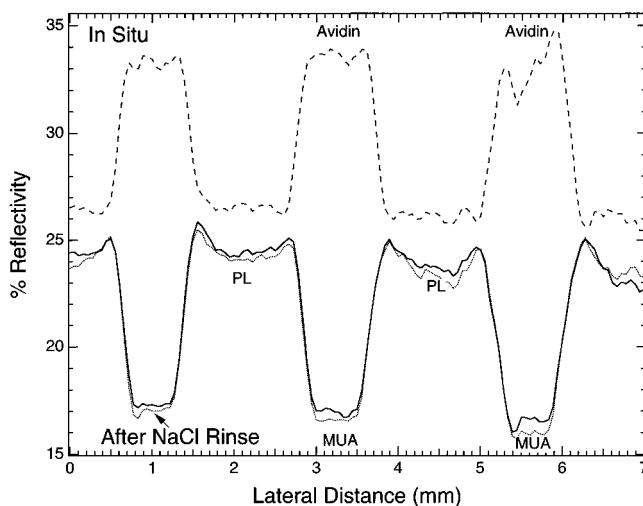
Figure 9. Line profiles measured in situ for avidin adsorption onto a patterned MUA/PL surface and the subsequent removal of avidin by high electrolyte concentration. The solid line is the %R from a MUA/PL surface imaged in buffer, and the dashed line is taken after exposure of the sample to a pH = 8.5 avidin solution and rinsing with buffer. The dotted line is the %R measured in the buffer after exposure of the sample to 2 M NaCl (pH = 8.5). The dotted line shows that a high concentration of electrolyte will remove all of the avidin from a MUA/PL surface, as expected for electrostatically bound avidin.

smaller differential reflectivity for a given change in thickness than that observed ex situ. However, the qualitative results are the same: if an SPR imaging experiment is performed at a fixed angle just below the SPR minimum, then an increase in the %R is observed as avidin adsorbs onto the surface. Figure 8 plots the theoretical change in %R expected in situ as a biopolymer thin film having an index of refraction of 1.45 adsorbs onto the gold surface. At the fixed angle labeled "I" in Figure 7, the differential reflectivity increases linearly over the first 50 Å and then slowly levels out. In contrast, if an angle on the other side of the SPR minimum were chosen (labeled as "II" in Figure 7), an initial decrease in the %R would be observed upon adsorption of the polypeptide. If the SPR imaging measurements are performed at multiple fixed angles such as those plotted in Figure 7, then changes in effective film thickness can be calculated more reliably during an adsorption experiment, and the SPR imaging apparatus can be used to examine films over a wider range of thicknesses.

Figure 9 plots the line profiles from a series of in situ SPR imaging measurements on MUA/PL surfaces identical to those used in the ex situ experiments. Notice that the two areas on the MUA/PL surface show a smaller difference in %R in this in situ experiment than in the corresponding ex situ experiment (Figure 6), as predicted from the scanning SPR curves in Figure 7. As in the ex situ measurements, exposure of this surface to
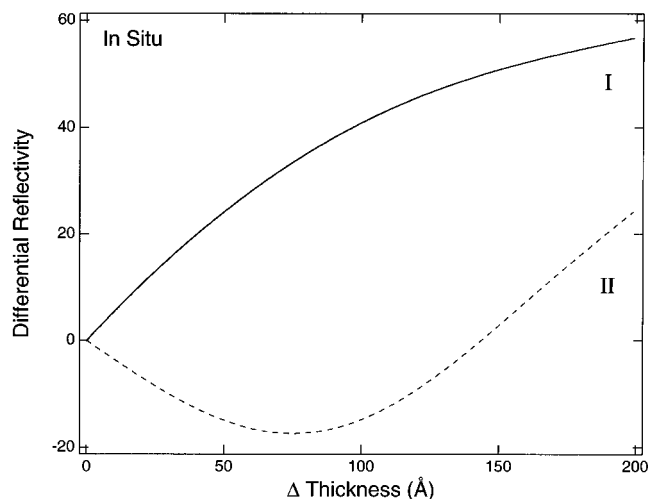
an avidin solution results in the strong adsorption of the protein avidin onto the MUA monolayer portions of the surface (dashed line). Using in situ measurements, the avidin adsorption is found to reach a constant level in about 5 min; this level of adsorption does not change when the avidin solution is replaced with pH = 8 buffer.

Also shown in Figure 9 is the line profile of the photopatterned SPR image after rinsing with a 2 M NaCl solution (dotted line). The line profile shows that the avidin monolayer has been completely removed upon exposure to a high-concentration salt solution due to the screening of the PL and MUA charges. This
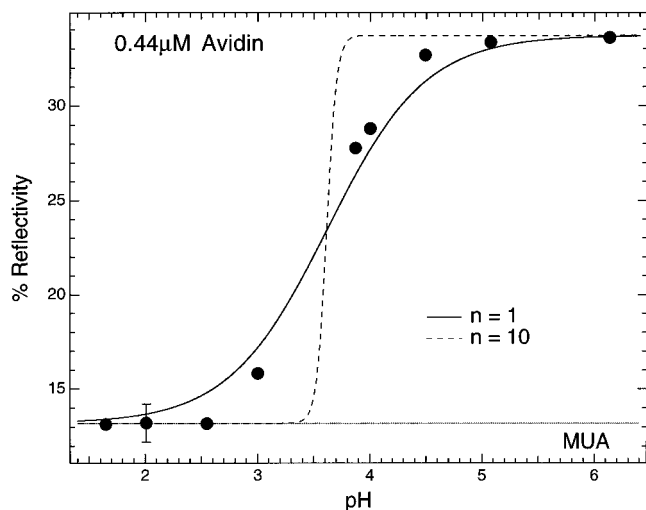
Figure 10. The % reflectivity measured from a MUA surface in equilibrium with a 0.44 μM avidin solution as a function of solution pH. At pHs below 2.5, no avidin adsorbs to MUA. This can be seen by the overlap of the circles below pH = 2.5 with the dotted line, where the dotted line shows the %R from MUA before exposure to avidin. At pHs greater than 5.0, the amount of avidin adsorption plateaus at a %R that corresponds to a full monolayer of avidin. This titration curve was fit to eq 3 for $n = 1$ and $K_{ads} = 550$ (solid line). The dashed line shows the theoretical curve if $n = 10$.

observation agrees with our previous assertion that the avidin is adsorbed electrostatically to the MUA monolayer. The rate of desorption of the avidin and the residual amount of the protein on the surface varied with the salt concentration; complete desorption of the monolayer occurred within 20 min for all NaCl solutions above 1.0 M.

An electrostatically adsorbed PL monolayer, when exposed to a high salt solution directly after deposition, will also completely desorb as expected. However, we have observed that, if the PL–MUA bilayer is heated at 100 °C for 1 h before exposure to a 2 M NaCl solution, little or no PL desorption is detected. We hypothesize that this irreversible binding of the PL–MUA bilayer is due to hydrogen bond formation caused by dehydration and/ or conformational changes which occur during heating. In the process of making the patterned MUA/PL samples (shown in Figure 5), the PL–MUA bilayers were heated, and for this reason we did not observe any loss of PL during the 2 M NaCl rinse shown in Figure 9.

Further in situ SPR imaging experiments were performed in order to examine the effect of solution pH on avidin adsorption to the MUA monolayer. As the pH is lowered, the carboxylic acid groups of the MUA monolayer should become protonated, and the electrostatically adsorbed avidin molecules should desorb. The %R measured for an avidin monolayer adsorbed to a MUA SAM from a 0.44 μM solution is shown as a function of pH in Figure 10; the data in this figure were obtained from a series of SPR imaging experiments of a MUA/PL surface. Above pH = 5.0, a full avidin monolayer is adsorbed onto the MUA SAM. However, below this pH, only partial avidin monolayers are observed, and by pH = 2.5, the avidin is completely removed from the surface. Further experiments (not shown) also indicate that avidin will completely desorb in a pH = 13 solution. Since this pH is significantly above the pI of avidin, this observation also supports the assertion that avidin is electrostatically adsorbed to the MUA SAM.

The data in Figure 10 resemble a titration curve with an "effective pK_a" of 3.6, the pH at which approximately 50% of a full avidin monolayer adsorbs to the MUA surface. However, this is not the pK_a of the MUA monolayer. The structure and pK_a of the MUA monolayer have been characterized extensively,[36–40] and a pK_a of approximately 6.5 has been inferred from contact angle measurements performed on both MUA[41] and mixed monolayers of MUA and nonanethiol.[42] This difference of 3 pH units between the pK_a for a MUA monolayer and the effective pK_a observed for the adsorption of an avidin monolayer can be explained on the basis of the coupling of the K_a for MUA and the ion pairing constant between avidin and the MUA monolayer. The adsorption of avidin onto a MUA SAM can be described by the following chemical equilibrium:

$$H_nX + Av^{M+} \Leftrightarrow AvX^{(M-n)+} + nH^+ \qquad K_{ads} \qquad (1)$$
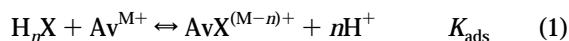
where X represents an avidin adsorption site on a MUA SAM, Av is avidin, n is the number of carboxylate ions that interact with an adsorbed avidin molecule, and the equilibrium constant K_{ads} is the overall adsorption coefficient. Applying the standard Langmuir assumption that the rates of adsorption and desorption are proportional respectively to the number of occupied and unoccupied sites leads to the following expression for K_{ads}:

$$K_{ads} = \frac{\theta(a_{H+})^n}{(1 - \theta)a_{Av}} \qquad (2)$$

where θ is the relative surface coverage of avidin normalized to the maximum possible avidin surface coverage, Γ/Γ_{max}. Solving eq 2 for θ as a function of hydrogen ion activity results in eq 3:

$$\theta = \left(1 + \frac{(a_{H+})^n}{K_{ads}a_{Av}}\right)^{-1} \qquad (3)$$

The overall adsorption coefficient is a combination of the K_a for a MUA monolayer and the equilibrium constant K_{ip} for the ion pairing between avidin and the MUA SAM:

$$H_nX \Leftrightarrow X^{n-} + nH^+ \qquad K_a{}^n \qquad (4)$$

$$X^{n-} + Av^{M+} \Leftrightarrow AvX^{(M-n)+} \qquad K_{ip} \qquad (5)$$
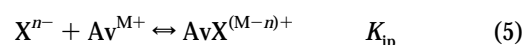
Combining eqs 4 and 5 to produce eq 1 results in an overall adsorption coefficient $K_{ads} = K_a{}^nK_{ip}$. The fact that K_{ads} can be described as a combination of K_a and K_{ip} can be used to explain the difference between the reported pK_a for MUA and the effective pK_a obtained from the data in Figure 10.

The effect of ion pairing on this difference can be seen most clearly by rearranging eq 3 and solving for the pH at which the

(36) Smith, E. L.; Alves, C. A.; Anderegg, J. W.; Porter, M. D.; Siperko, L. M. *Langmuir* **1992**, *8*, 2707–2714.
(37) Chidsey, C. E. D.; Loiacono, D. N. *Langmuir* **1990**, *6*, 682–691.
(38) Duevel, R. V.; Corn, R. M. *Anal. Chem.* **1992**, *64*, 337–342.
(39) Kepley, L. J.; Crooks, R. M.; Ricco, A. J. *Anal. Chem.* **1992**, *64*, 3191–3193.
(40) Sun, L.; Crooks, R. M.; Ricco, A. J. *Langmuir* **1993**, *9*, 1775–1780.
(41) Creager, S. E.; Clarke, J. *Langmuir* **1994**, *10*, 3675–3683.
(42) Bain, C. D.; Whitesides, G. M. *Langmuir* **1989**, *5*, 1370–1378.

relative avidin surface coverage is one-half (pH$_{\theta=0.5}$):

$$pH_{\theta=0.5} = pK_a - \frac{1}{n} \log(K_{ip}a_{Av}) \qquad (6)$$

Equation 6 predicts a shift of the effective pK_a to more negative values as ion pairing becomes important. This shift depends on the values of n, K_{ip}, and a_{Av}. The value of n also determines the slope at $\theta = 0.5$ for a fit of the data to eq 3. From the relative size and charge of avidin as compared to those of a MUA molecule, it is reasonable that a single avidin interacts with perhaps 10 surface carboxylate groups. However, the slope of the theoretical fit at $\theta = 0.5$ is much too steep if $n = 10$ is used (as shown by the dashed line in Figure 10), and an unreasonable value for K_{ip} of 10^{35} is calculated. A much better fit to the data and a more reasonable K_{ip} are obtained if n is set equal to 1 or 2. A fit using $n = 1$ and $K_{ads} = 550$ is shown as the solid line in the figure. From this fit, a K_{ip} of 1.7×10^9 can be calculated if one uses the approximate value p$K_a = 6.5$ for MUA. Although this is a much more reasonable K_{ip} value for the nonspecific interaction of avidin and MUA, it is still somewhat larger than that expected for carboxylate ion pairing constants. However, it is much weaker than the formation constant for the specific reaction of avidin with biotin ($K_{binding} = 10^{15}$).[43] The facts that the calculated K_{ip} is significantly larger than expected, and that a Langmuir adsorption isotherm fits the data only with the physically unreasonable value $n = 1$, indicate that avidin adsorption onto a MUA monolayer is not described well by the Langmuir model. This failure of the Langmuir model is understandable since the Langmuir model makes assumptions that are not necessarily expected to be true for electrostatic adsorption processes on MUA monolayers. Electrostatic interactions are long range; therefore, an adsorbed avidin molecule will interact with the entire MUA surface and not a specific site as assumed in the Langmuir model. In addition, lateral protein–protein interactions may exist between adsorbed molecules at higher surface coverages. Despite the fact that the avidin ion pairing adsorption onto a MUA surface can be described more accurately by more complex models,[44–46] eq 6 shows that the simple Langmuir model *does* account for the shift between the approximate pK_a for MUA of 6.5 and the effective pK_a of 3.6 for avidin adsorption onto MUA by considering the strong ion pairing interactions between the protein and the charged surface.

Molecular Weight Dependence of PL Adsorption. Another factor that affects the electrostatic adsorption of polypeptides to surfaces is the number of monomers in the polypeptide. In a final set of SPR imaging experiments, this effect is examined by measuring the amount of PL adsorbed to MUA as a function of PL molecular weight. We have previously observed in ex situ measurements that PL molecules with an average of 67 lysine residues will form a full monolayer on a MUA surface from a pH = 8.5 solution but that lysine monomers will not adsorb at this pH.[15] Figure 11 shows the results of a series of in situ SPR imaging experiments in which the amount of PL adsorbed onto a MUA monolayer was determined for a series of solutions with an average PL length that varied from 1 to 270 lysine residues. In
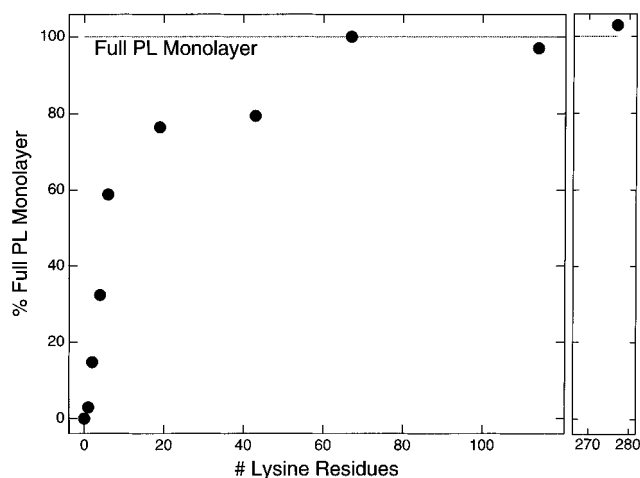
(43) Green, N. M. *Avidin in Protein Chemistry*; Academic Press: New York, 1975; pp 85−133.
(44) Yoon, B. J.; Lenhoff, A. M. *J. Phys. Chem.* **1992**, *96*, 3130−3134.
(45) van der Schee, H. A.; Lyklema, J. *J. Phys. Chem.* **1984**, *88*, 6661−6667.
(46) Muthukumar, M. *J. Chem. Phys.* **1987**, *86*, 7230−7235.

Figure 11. The percentage of a full PL monolayer electrostatically adsorbed onto MUA as a function of the molecular weight measured in pH = 8.5 solutions, each with a constant lysine residue concentration of 0.7 mM. Percent reflectivities were obtained from a surface patterned with stripes of MUA and mercaptoundecanol (MUD). The percentage of a full PL monolayer was obtained by normalizing the difference in %*R* seen for each length PL on MUA to the maximum PL coverage. No adsorption is seen for L-lysine, but the percent of adsorption increases rapidly with polymer chain length, until a full monolayer of PL is adsorbed for chain lengths longer than 67 monomer units.

these experiments, a constant lysine residue concentration of 0.7 mM was maintained in each solution. Each point in Figure 11 was obtained by measuring the amount of PL adsorbed onto the MUA portions of a gold thin film that was photopatterned with areas of MUA and MUD. A striped MUA/MUD surface was used in these experiments since PL does not adsorb onto a MUD SAM; therefore, the %*R* of the MUD surface could be used as an internal standard. With these MUA/MUD surfaces, we were able to monitor the very small changes in the %*R* observed for the partial monolayers formed on the MUA monolayer from low molecular weight PL. The MUA/MUD surface was regenerated between exposures to the various PL solutions by rinsing with an acidic (pH = 2) buffer. The percentage of a full monolayer (shown in Figure 11) was obtained by normalizing the %*R* measured for each length PL on MUA to the maximum PL coverage. The amount of adsorbed PL increases quickly from no observable adsorption for lysine monomers to 60% of a monolayer for PL with six residues and then levels off until a plateau is reached at full monolayer coverages for chain lengths above 67 lysine residues. Since the lysine residue concentration is held constant during these experiments, the increased PL adsorption with chain length is due solely to an increased affinity between the longer PL molecules and the MUA surface. It was also determined that monolayers formed from PL solutions with average chain lengths greater than 19 residues showed no desorption when rinsed with a buffer solution, but some loss of PL was observed for the shorter PL chains upon rinsing. This indicates that, in addition to the adsorption coefficient, the adsorption kinetics are also affected by the molecular weight of the polypeptide.

The process of electrostatic polymer adsorption and its dependence on molecular weight have been examined previously for various polyelectrolytes.[47,48] In particular, the adsorption of

(47) Papenhuijzen, J.; Fleer, G. J.; Bijsterbosch, B. H. *J. Colloid Interface Sci.* **1985**, *104*, 530−539.

PL has been observed on AgI, silica, and polystyrene latex surfaces.[14,49−51] The molecular weight dependence observed for PL adsorbed onto MUA in the SPR experiments reported here is in good qualitative agreement with the measurements of van der Schee and Lyklema for poly-L-lysine adsorbed onto modified AgI surfaces.[49] An increase in adsorption with molecular weight for shorter chain lengths is common for both charged and uncharged polymers and is due to an increase in surface affinity. However, as the molecular weight is increased further, a plateau at monolayer coverage is typically observed for polyelectrolytes and arises from electrostatic repulsion inhibiting the formation of multilayers.[48]

SUMMARY AND CONCLUSIONS

The technique of SPR imaging has been used in this work to investigate the electrostatic adsorption of proteins and polypeptides onto chemically modified gold surfaces. SPR imaging is well-suited for these studies because (i) biopolymer adsorption onto a photopatterned array of several chemically different surfaces can be observed simultaneously with this technique, (ii) any sample-to-sample variations in both ex situ and in situ differential adsorption measurements can be eliminated by using these photopatterned surfaces, and (iii) quantitative adsorption information can be readily extracted from the resulting SPR images and line profiles. Through a set of ex situ SPR imaging experiments of avidin and α-acid glycoprotein adsorption onto patterned MUA/PL surfaces, it has been shown that the pI of the two proteins is a key factor in controlling their adsorption onto charged surfaces. These results suggest that, in the future, SPR imaging experiments may be used to distinguish proteins on the basis of their pI. The electrostatic adsorption of avidin to a MUA monolayer has been probed in further detail with a series of in situ SPR imaging experiments of avidin desorption in solutions with either high electrolyte concentration or extreme pH. Further experiments investigating the effect of solution pH on the avidin adsorption equilibrium result in an "effective pK_a" for the avidin adsorption onto MUA of 3.6. This value is lower than the pK_a of the MUA monolayer ($\approx$6.5), and the difference can be accounted for by strong ion pairing interactions between avidin and the MUA SAM.

The dependence of electrostatic polypeptide adsorption on chain length was also investigated using in situ SPR imaging by measuring the adsorption of different length poly-L-lysine molecules onto a MUA surface. The amount of PL adsorption was found to increase quickly from no adsorption for lysine monomers to full monolayer coverage for PL having more than 67 lysine residues. This increase in adsorption with molecular weight is due to an increased affinity between the MUA surface and the longer PL molecules, and the plateau seen at higher molecular weights is a result of the electrostatic repulsion between PL molecules, which inhibits the formation of multilayers. Future experiments will employ SPR imaging to monitor protein adsorption onto surfaces with multiple areas of different charge densities and to investigate the hybridization adsorption of complementary DNA molecules onto oligonucleotide monolayers at chemically modified gold surfaces.

(48) Cohen-Stuart, M. A.; Fleer, G. J.; Lyklema, J.; Norde, W. *Adv. Colloid Interface Sci.* **1991**, *34*, 477−535.
(49) van der Schee, H. A.; Lyklema, J. In *The Effect of Polymers on Dispersion Properties*; Fadros, T. F., Ed.; Academic Press: London, 1982; pp 81−100.
(50) Fernandez, V. L.; Reimer, J. A.; Morton, M. D. *J. Am. Chem. Soc.* **1992**, *114*, 9634−9642.
(51) Bonekamp, B. C.; Lyklema, J. *J. Colloid Interface Sci.* **1986**, *113*, 67−75.